Supplementary Materials: Thermal and Physical Investigations into Lake Deepening Processes on Spillway Lake, Ngozumpa Glacier, Nepal

Ulyana Horodyskyj

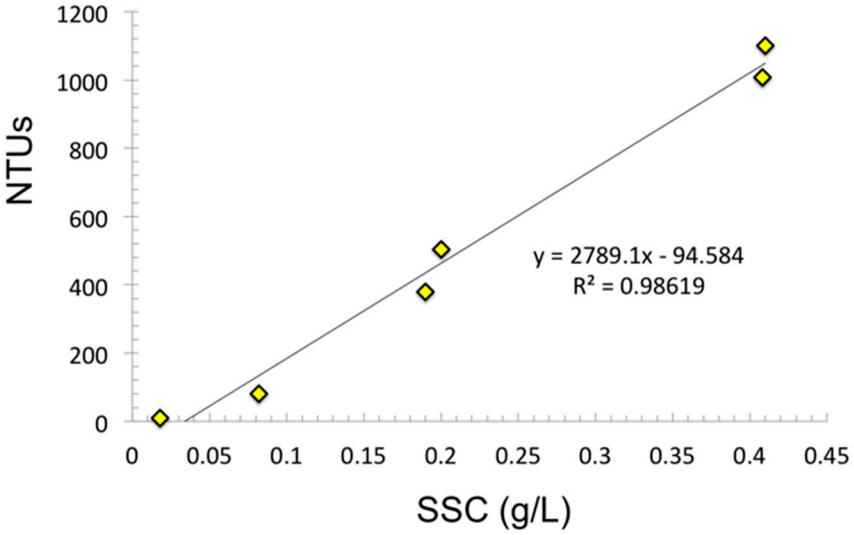

Figure S1. Conversion of field and lab-measured turbidity values (NTU) to suspended sediment concentration (SSC) in g/L.

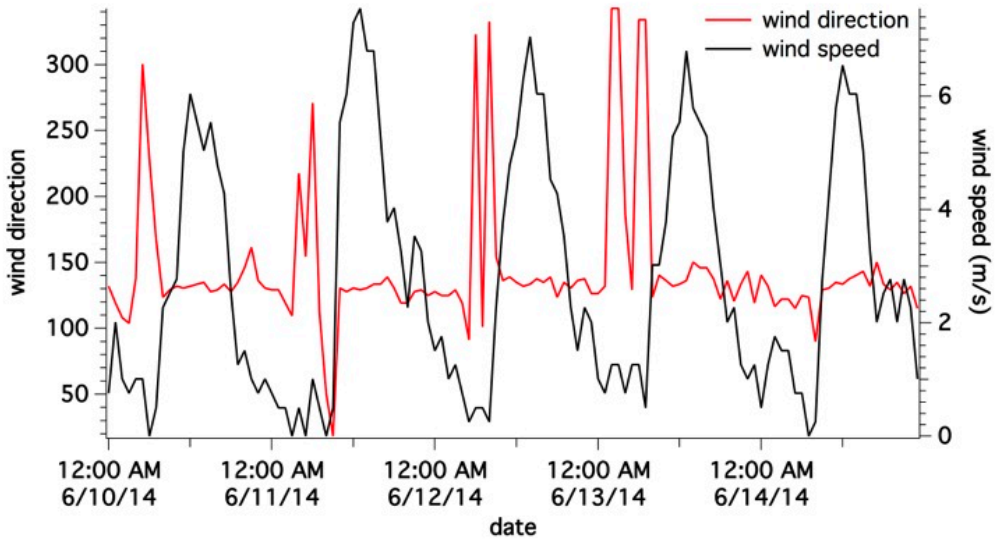

Figure S2. Wind direction (red) and wind speed (black) data subset from June 2014. General trends include highest wind speeds (>5 m/s) in the afternoon, starting at 12 p.m. During the day, wind direction (~130°) comes via valley winds from the southeast. At night, wind direction (~250–300°), and speed (<2 m/s) switch to weaker northwesterly mountain downdrafts.

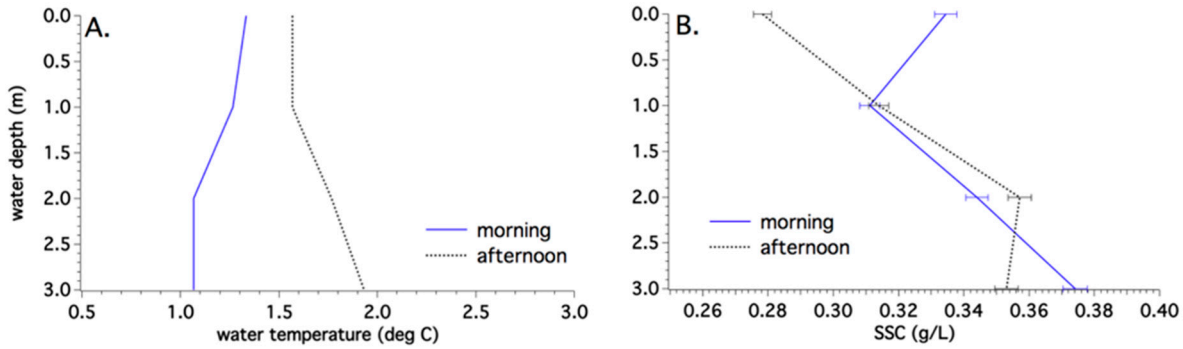

Figure S3. SW sub-basin temperature (**A**) and suspended sediment concentration (**B**) with depth. Shallow depth leads to much higher overall temperatures from top to bottom. Similar to the other sub-basins, SSC increases with depth indicating a stable density structure.

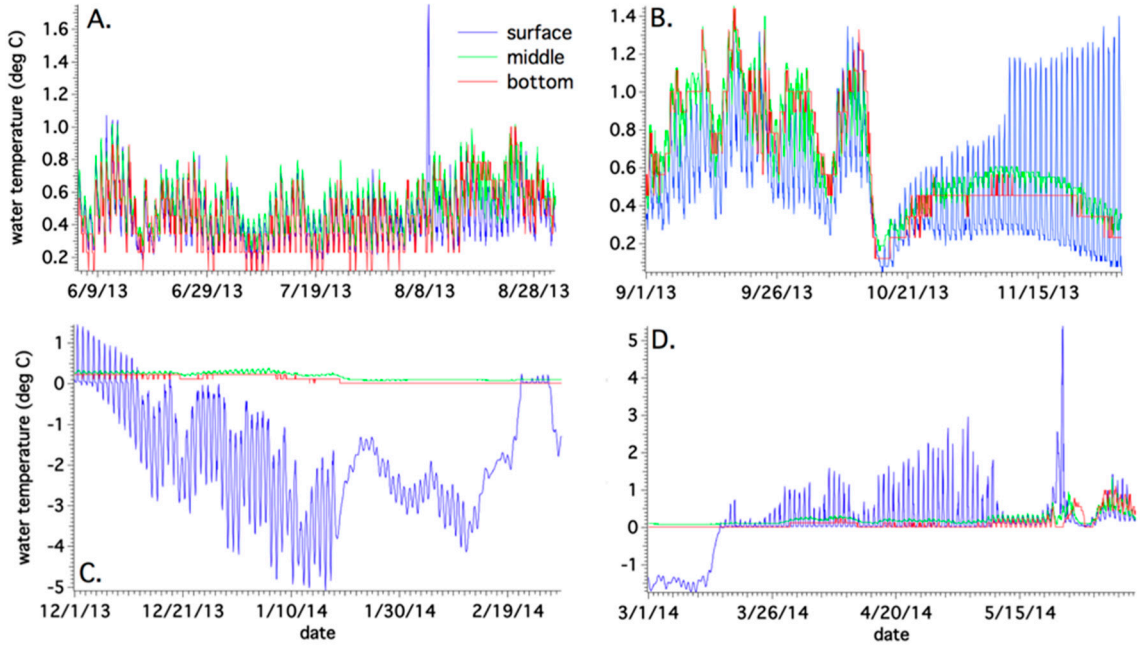

Figure S4. Seasonal temperature variations in NW sub-basin buoy location for the monsoon (**A**); fall (**B**); winter (**C**) and spring (**D**). Surface in blue; middle in green; bottom in red.

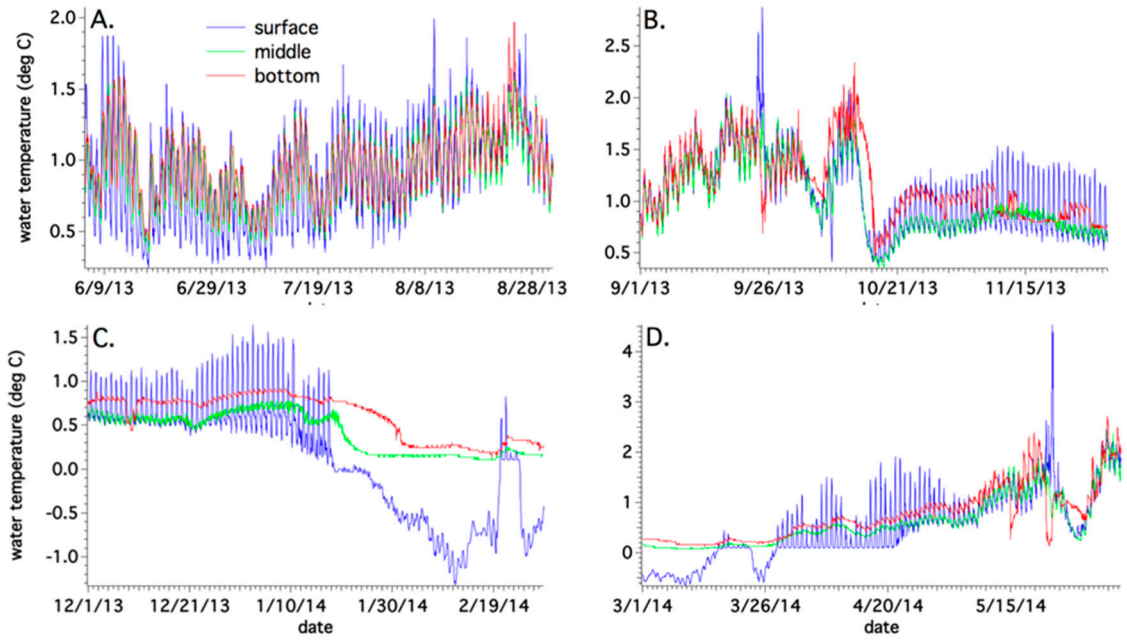

Figure S5. Seasonal temperature variations in NE sub-basin buoy location for the monsoon (**A**); fall (**B**); winter (**C**) and spring (**D**). Surface in blue; middle in green; bottom in red.

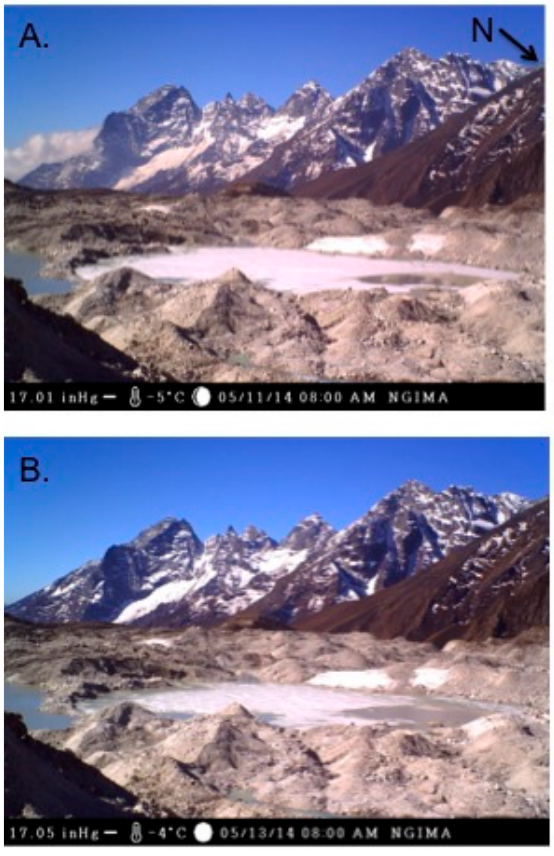

Figure S6. Time-lapse sequence of the Main sub-basin thaw from 11 May to 19 May 2014.

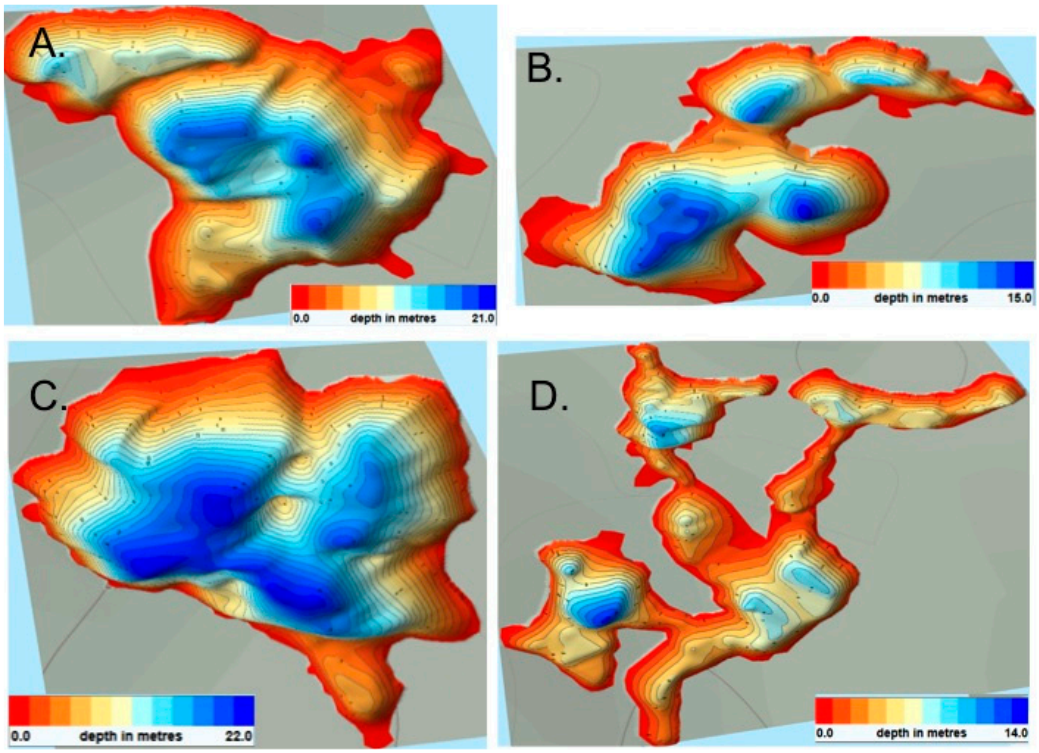

Figure S7. Derived 3D models of the sub-basins, with 2–3 × vertical exaggeration. NW sub-basin (**A**); NE sub-basin (**B**); Main sub-basin (**C**) and SW sub-basin with surroundings (**D**).

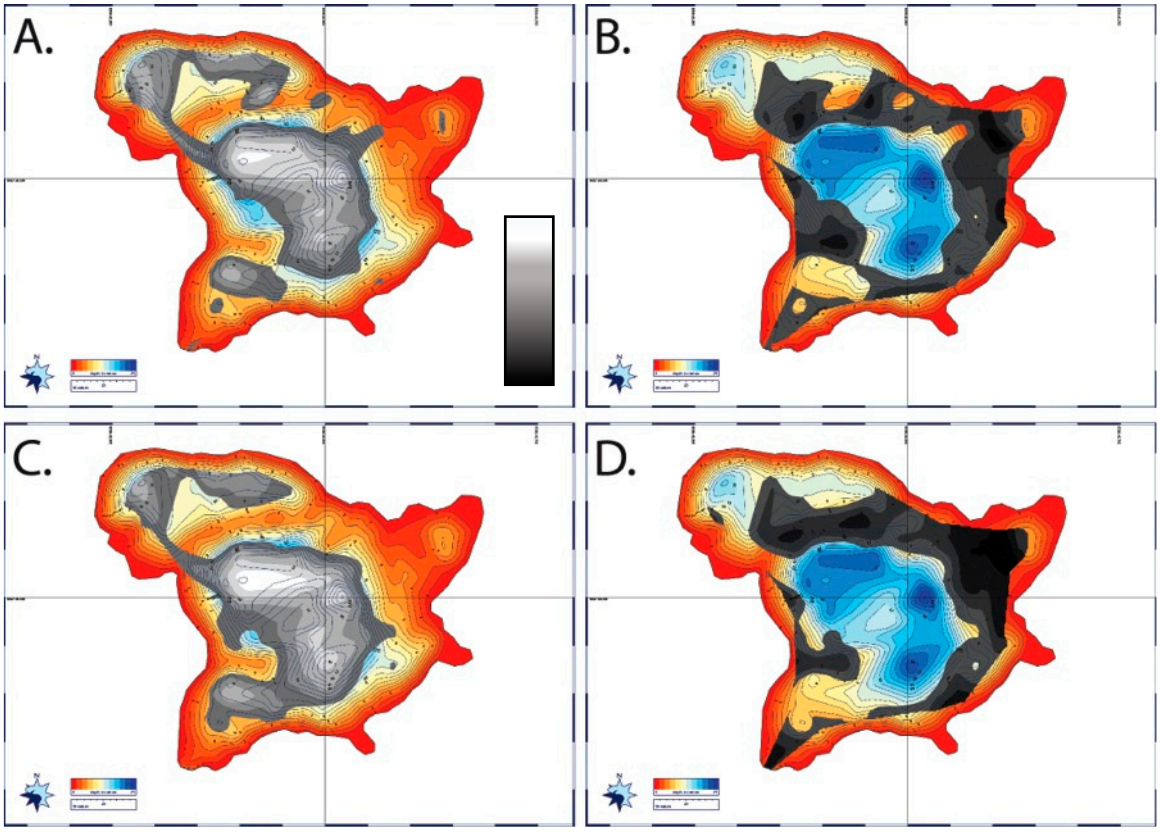

Figure S8. NW sub-basin roughness and hardness maps, generated from E1 and Peak Sv acoustic backscatter values. Smooth (**A**); rough (**B**); soft (**C**) and hard (**D**) are shown.

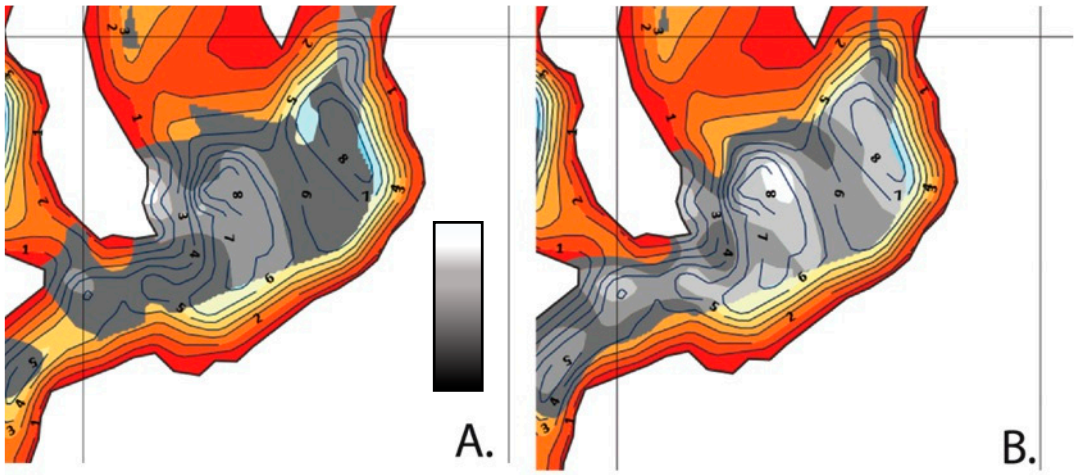

Figure S9. Zoom-in of SW sub-basin roughness and hardness maps, generated from E1 and Peak Sv acoustic backscatter values. Smooth (**A**) and soft (**B**) are shown, showing good overlap and consistent with high sedimentation rates in this region.

Figure S10. Frozen-over upwelling (December 2013) in the northeastern part of Main basin, Spillway Lake.

Table S1. Six samples (one from each sub-basin (with repeat done for NE sub-basin); and two different locales within the Main sub-basin) and the average values for thermal conductivity (k), thermal resistivity (rho), volumetric heat capacity (C) and thermal diffusivity (D), with error.

Samples (rock/mud mix)	K (W/(m·K))	RHO (°C·cm/W)	C (MJ/(m³·K))	D (mm²/s)	Error
NW sub-basin	1.964	50.9	2.707	0.726	0.0058
NE sub-basin	1.663	60.1	2.686	0.619	0.005
Main sub-basin	1.764	56.7	2.572	0.686	0.008
Main sub-basin	1.813	55.1	2.768	0.655	0.009
NE sub-basin (repeat)	1.663	60.1	3.098	0.537	0.0067
SW sub-basin	1.868	53.5	2.464	0.758	0.0044
Average	**1.789**	**56.067**	**2.716**	**0.664**	**0.006**